International Journal of Coal, Geology and Mining Research
Vol.4, No.1, pp.1-16, 2021
Published by European Centre for Research Training and Development UK

Geochemical and Mineralogical Investigation of Sub-Recent Formation Silica Sand to Evaluate its Suitability for Industrial Utilization, Thar Block II, Pakistan

Ali Iqtidar[1*], Nawab Muhammad Abid Zubair[1]
[1]Geology and Hydro-Geology Division, Sindh Engro Coal Mining Company, Thar Block II, Pakistan

Citation: Ali Iqtidar, and Nawab Muhammad Abid Zubair (2022) Geochemical and Mineralogical Investigation of Sub-Recent Formation Silica Sand to Evaluate its Suitability for Industrial Utilization, Thar Block II, Pakistan, *International Journal of Coal, Geology and Mining Research*, Vol.4, No.1, pp.1-16

ABSTRACT: *The region of Thar Parker which is located at the eastern part of Sindh province, historically consists of three underground aquifers namely 1 – Dune sand aquifer, 2 - Coal seam roof aquifer and 3 – Coal seam floor aquifer. Present study is aimed at the geochemical and mineralogical investigation of silica sand from coal seam roof aquifer layer to evaluate its suitability for industrial application since it is found at relatively shallower depth and its pressure has been nearly reduced due to ongoing mining and dewatering operations at Thar Block II. The grain size distribution curve reveals that the aquifer sand is mainly contributed of fine to medium grain sand with its permeability ranges from $6.32E^{-5}$-$3.60E^{-4}$m/s. The geochemical analysis indicates that the SiO_2 content of aquifer silica sand ranges from 47.72-85.27% and has undergone extensive degree of chemical weathering which is calculated from chemical index of alteration (79.04-88.40), TiO_2/Al_2O_3 ratio (8.16-4.02) and index compositional variance (0.13-0.46). The mineralogical assessment suggest that aquifer sand layer is primarily composed of rich to intermediate quartz with secondary amount of feldspar and clay minerals. The SiO_2 content of aquifer sand has been compared with the standard industrial requirements for typical silica sands which reveals that the SiO_2 content of studied sand shall be enhanced using various beneficiation techniques in order to utilize it industrially and commercially.*

KEYWORDS: silica sand; geochemistry; mineralogy; coal seam roof aquifer; grain size analysis; industrial utilization

INTRODUCTION

Sand with particularly high silica levels that is used for purposes other than construction is referred to as silica sand or industrial sand. Silica sands has got the most diversified applications among all the non-metallic minerals due to its common occurrence around the world and distinctive physical characteristics like hardness, chemical composition and heat resistance [Sundararajan et al., 2009]. Raw silica can be usually used in foundry, ceramics, sand blasting, water filtration, pigments, hydraulic fracturing and propping in the oil industry [Boussaa et al., 2016].

Thar Coal Field

The Thar coal field is situated at south-eastern part of Sindh, where about 176 Bt of total lignite has been explored [Rehman et al., 1993]. Since the coal sequence in Thar Coal Field is bounded by thick groundwater bodies [Kazmi, 1985], which are composed of silica sand and are laterally

continuous all over the Thar region. At present, 13 coal blocks have been demarcated in Thar district out of which Block II covers an area of 95.5 Km2 and coal resources of 2.4 Bt [Fig. 01].

The Thar coal field is situated at south-eastern part of Sindh, where about 176 Bt of total lignite has been explored [Rehman et al., 1993]. Since the coal sequence in Thar Coal Field is bounded by thick groundwater bodies [Kazmi, 1985], which are composed of silica sand and are laterally continuous all over the Thar region. At present, 13 coal blocks have been demarcated in Thar district out of which Block II covers an area of 95.5 Km2 and coal resources of 2.4 Bt [Fig. 01].

The present study emphases on the geochemical and mineralogical investigation of silica sand from Thar Block II coal seam roof aquifer of Sub-Recent formation in order to evaluate its suitability for industrial utilization and economic potential.

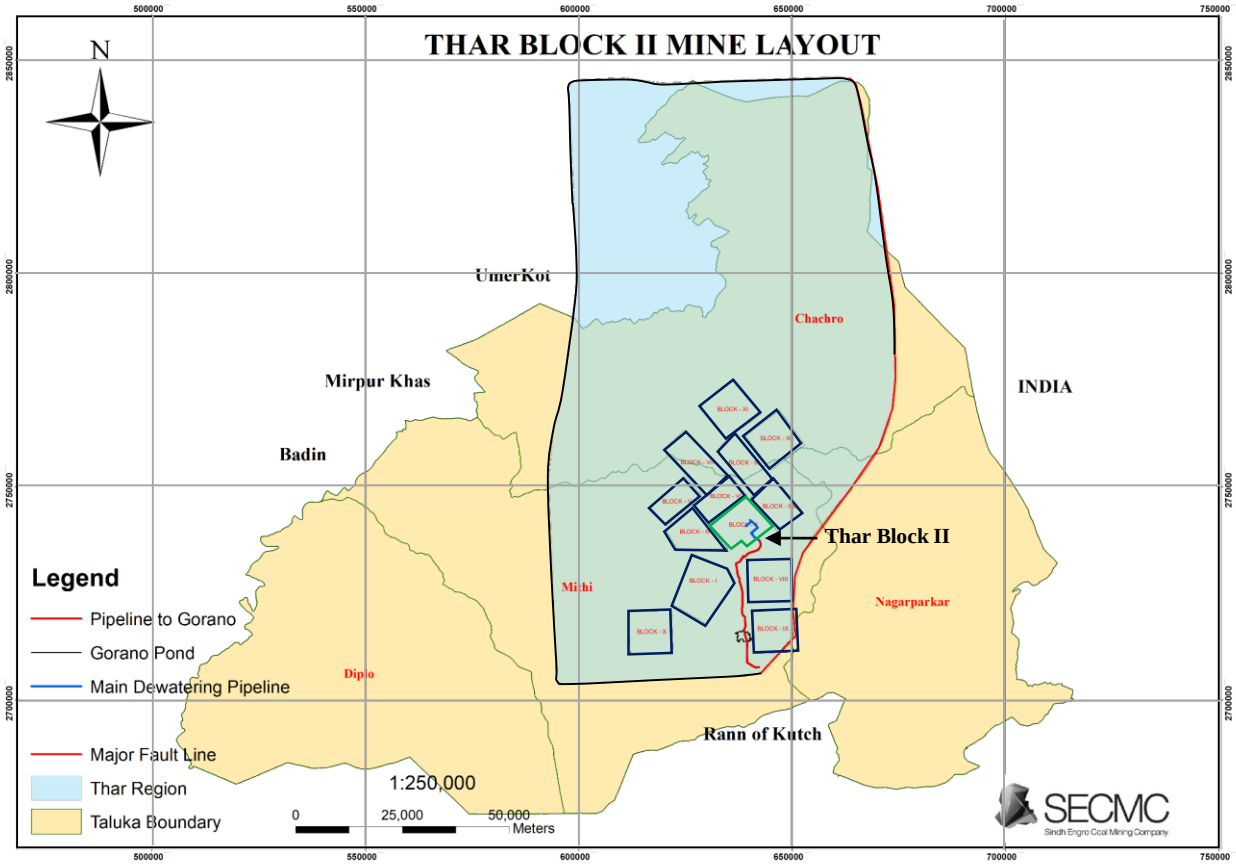

Fig. 1. Location map of Thar Coal Block II, Thar District, Sindh

Mine Development Plan

Block II mining operations are ongoing since Apr 2017 with the aim to produce 3.8 Mt per annum of coal as part of first phase. Since all the coal seams/sequence are interbedded between coal seam roof and floor aquifer, continuous depressurizing and dewatering (underground and surface) of these aquifers is of vital importance in order to mine Thar coal. Coal seam roof aquifer which is generally found at relatively shallower depth i.e. 125m with an average thickness of 12m has already been depressurized and dewatered at the first phase of Block II mine. However, aquifer depressurizing and dewatering will be continued since mining

operations in Thar Block II are planned to expand up to 20 Mt per annum coal production which will last for more than 30 years. The overall volume of coal seam roof aquifer is 1,065 Mm^3 which contributes to 8% of the total overburden material present within Thar coal Block II boundary.

GENERAL GEOLOGY

The study area, Block II generally consists of various sedimentary formations which are overlaid on granitic igneous basement. These sedimentary bodies are separated by regional unconformities and groundwater aquifers [Table 1].

Table 1 Generalized stratigraphic column of Block II, Thar District, Sindh

Formation/Aquifer	Age	Top Elevation (AMSL)	Thickness (m)	Lithology
Dune Sand Formation	Recent	80 to 70	50 - 55	Sand, silt
Dune Sand Aquifer	Recent	25 to 20	5 - 6	Quarzitic Sand
Alluvial Deposits	Sub-Recent	20 to 15	70 - 80	Sand, siltstone, claystone
Sand Lenses	Sub-Recent	18 to -6	4 - 5	Fine sand
Coal Seam Roof Aquifer	Sub-Recent	-45 to -55	10 - 15	Quarzitic Sand
Bara (Coal Bearing) Formation	Eocene	-60 to -70	80 - 90	Claystone, sand, coal, carbonaceous claystone
Coal Seam Floor Aquifer	Eocene	-110 to -120	30 - 40	Quarzitic Sand
Basement Complex	Precambrian	-	-	Granite, Diorite

Dune sand aquifer with relatively low thickness and much localized lateral extent [Jianmin et al., 2010] is not considered economically viable in the present study. The coal seam roof and floor aquifers are dominantly composed of quartz rich silica sand. The present study is aimed on the industrial evaluation of coal seam roof aquifer since it is found at relatively shallower depth and its pressure has been nearly reduced due to ongoing mining and dewatering operations at Block II.

MATERIAL AND METHODS

The 14m thick coal seam roof aquifer layer was vertically sub-divided into 7 zones (each approx. 2m thick) in order to collect representative samples from top to bottom covering complete coal seam roof aquifer layer [Table 2]. The collected samples were tested for grain size analysis and elemental oxides composition using appropriate analytical techniques.

Table 2 Categorization of coal seam roof aquifer layer, Block II, Thar District, Sindh

Aquifer Layer Categorization		Sample ID	Top Elevation (AMSL)	Bottom Elevation (AMSL)	Sample Thickness (m)
Upper	A	01	-47.12	-49.25	2.13
	B	02	-49.25	-50.69	1.44
Middle	C	03	-50.69	-52.24	1.56
	D	04	-52.24	-54.03	1.79
	E	05	-54.03	-55.94	1.92
Lower	F	06	-55.94	-58.13	2.19
	G	07	-58.13	-60.13	2.01

Grain Size Distribution

Each of the representative sample was oven dried at 105 ^{0}C until constant mass was achieved. The oven dried samples were manually sieved through different size fractions to determine the grain size distribution of the coal seam roof aquifer layer.

Geochemical Analysis

The collected raw samples were crushed into small pieces and mixed thoroughly followed by coning and quartering. The pulverized sample powder was sent to the Centralized Science Laboratory, University of Karachi for the determination of major and minor elemental oxides using JEOL JED-2300 Scanning Electron Microscope equipped with Energy Dispersive Spectroscopy (SEM-EDS) which provides chemical analysis of the field of view or spot analyses of minute particles. More than 90 elements can be detected with low-atomic number detector using the SEM/EDS technique. Samples were analysed systematically in three scans by producing a continuous series of photomicrographs which ranges from X5000 to X12000 in cross-sectional view, extending from the crust surface into the substrate of the rock samples. The elemental composition of each constituent observed in the photomicrographs was ascertained using EDS spot

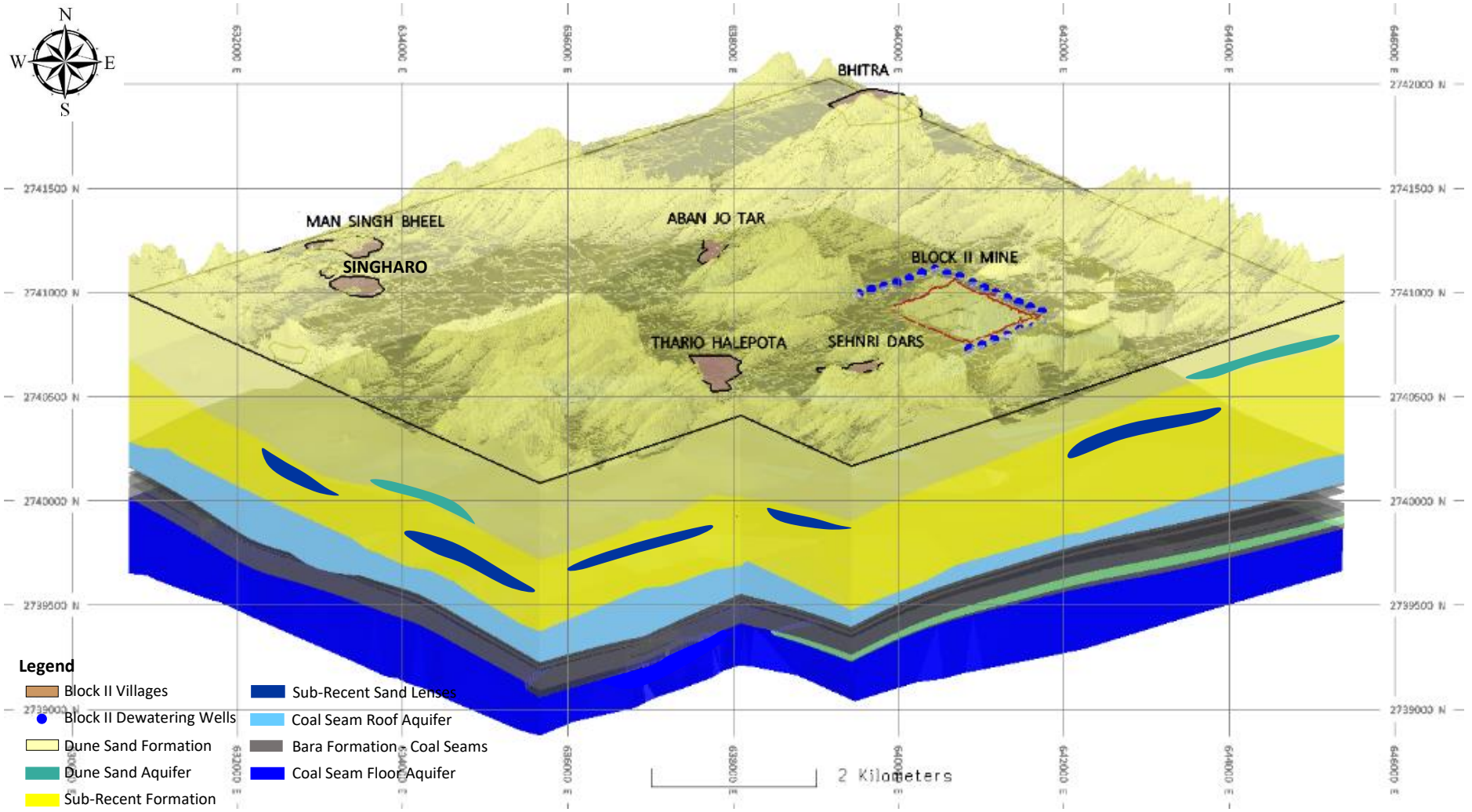

Fig. 2. 3D Geological model representing underground water bodies at Thar Coal Block II, Thar district, Sindh

analysis which was then marked directly on the photomicrograph, creating a continuous, high magnification compositional/morphological map of the crust in cross section. The pixel of all SEM images is 1280 * 960.

RESULTS AND DISCUSSIONS

Each of the 7 sand samples were classified in order to evaluate the distribution trend of coal seam roof aquifer layer in terms of its grain size, geochemistry and mineralogy.

Grain Size Analysis

Aquifer Categorization – Soil Type

Grain size analysis is generally used to categorize and classify siliciclastic rocks (conglomerate, sandstone, siltstone and claystone) in terms of its grain size distribution [Folk, 1951]. Grain size distribution plot of coal seam roof aquifer sample reveal that major proportion of all the samples fall between mesh no. 200 and 10 indicating that the coal seam roof aquifer layer is mainly contributed of fine to medium grain sand [Fig. 3]. Moreover, soil type

of each of the 7 zones of aquifer layer has also been identified based on the retaining percentage from the grain size analysis of studied samples [Table 3].

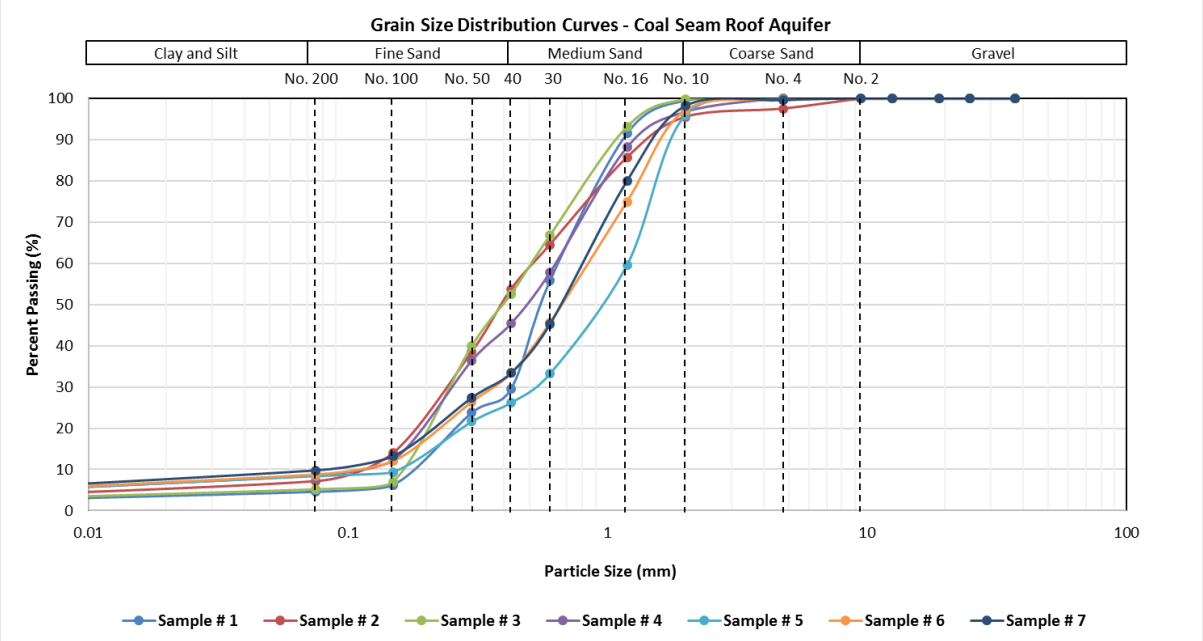

Fig. 3. Grain size distribution curve of coal seam roof aquifer samples, Thar Coal Block II

Aquifer Categorization – Permeability

Grain size distribution is widely used to evaluate the permeability which is one of the important and frequently used property of soil [Onur, 2014]. Permeability is a complex property that is controlled by physical properties of both the soil and the permeating fluid [DeGroot et al., 2012]. To calculate the permeability values of coal seam roof aquifer layer samples in the present study, Beyer's equation was used which has the form:

$K = C * (D_{10})^2$

From the above equation, the empirical term C is $4.5x10^{-3}$log (500/Cu). The effective diameter D_{10} is material finer than 10% in mm, Cu is the uniformity coefficient D_{60}/D_{10}, and K is hydraulic conductivity also called permeability in meters per second. The calculations reveal [Table 3] that the permeability values of coal seam roof aquifer samples range from $6.32E^{-5}$-$3.60E^{-4}$m/s. In addition, the uniformity coefficient (Cu) values of studied samples indicate that the coal seam roof aquifer layer composed of well graded soil particles in which smaller grains tend to fill the voids between larger grains [10]. The uniformity coefficient (Cu) is an important shape factor that represents the degree of sorting of a soil and indicates the slope of the grain size distribution curve [Mitchell and Soga, 2005].

Geochemistry

Relative abundance of 07 aquifer sand samples and mean values are listed in Table 4. The results reveal that the uppermost zone A of aquifer layer contains highest SiO_2 content of 85.27% while it significantly reduces downward to the lowermost zone G showing least amount of SiO_2 content i.e. 47.72%. In addition, high variation of Al_2O_3 [9.55-40.21%] concentration is observed in aquifer sand samples

Table 3 Classification of coal seam roof aquifer layer based on soil type and permeability (k), Thar Coal Block II,

Aquifer Layer Categorization		Sample ID	Retain Percent (%) - Mesh Size									Soil Type	D_{10} (mm)	D_{60} (mm)	Cu	C	K (m/sec)
			No. 4	No. 10	No. 16	No. 30	No. 40	No. 50	No. 100	No. 200	Pan						
Upper	A	01	0.0	0.4	8.0	35.8	26.2	5.8	17.6	1.6	4.6	Medium Sand	0.18	0.72	4.0	$9.44E^{-3}$	$3.06E^{-4}$
	B	02	2.4	2.0	9.8	21.2	10.8	15.2	24.6	6.8	7.2	Fine Sand	0.12	0.60	5.0	$9.00E^{-3}$	$1.30E^{-4}$
Middle	C	03	0.0	0.2	6.6	26.4	14.2	12.6	33.0	1.8	5.2	Fine Sand	0.19	0.58	3.05	$9.96E^{-2}$	$3.60E^{-4}$
	D	04	0.0	3.2	8.6	30.4	12.4	9.0	24.2	3.6	8.6	Medium Sand	0.13	0.68	5.23	$8.91E^{-3}$	$1.51E^{-4}$
	E	05	0.2	3.8	36.4	26.4	7.0	4.6	12.2	1.0	8.4	Medium Sand	0.17	1.25	7.35	$8.25E^{-3}$	$2.38E^{-4}$
Lower	F	06	0.4	2.4	22.2	29.4	12.2	7.0	14.4	3.2	8.8	Medium Sand	0.13	0.85	6.54	$8.48E^{-3}$	$1.43E^{-4}$
	G	07	0.4	1.4	18.2	34.8	11.8	6.0	14.2	3.4	9.8	Medium Sand	0.09	0.83	9.22	$7.80E^{-3}$	$6.32E^{-5}$

whereas oxide contents of CaO [1.57-2.14%], Na_2O [0.31-4.49%] and K_2O [1.35-2.07%] is relatively much uniform. Fe_2O_3 [3.32%] is only reported in sample 02 while Chlorine content is detected only in sample 02, 05, 06 and 07.

Chemical Weathering

A good measure to characterize the chemical weathering intensity within a weathered soil profile is by calculating the chemical index of alteration [CIA, Nesbitt & Young, 1982], also called chemical index of weathering [CIW, Fedo et al., 1995]. It is the ratio of $Al_2O_3/Al_2O_3+CaO+K_2O+Na_2O]*100$. High CIA values (i.e. 75-100) indicate intensive weathering whereas low values (i.e. 60) indicate relatively low weathering in the area. The calculated CIA values of the studied aquifer sand samples range from 79.04-88.40 [Table 4].

These values (>75) indicate intensive chemical weathering in the study area and reflect that the coal seam roof aquifer sand have formed under tropical conditions [Nesbitt & Young, 1982].

Similarly, TiO_2/Al_2O_3 ratio can also be used to evaluate the degree of chemical weathering, since TiO_2 and Al_2O_3 are generally considered to be immobile chemical components in a weathering profile, the TiO_2 and Al_2O_3 contents are expected to gradually increase by accumulation, and the TiO_2/Al_2O_3 ratio will remain constant as the weathering proceeds [Nesbitt & Young, 1982; Scheffler et al., 2003; Nedachi et al., 2005]. Indeed, the immobile behaviour of Ti and Al is confirmed by the decreasing ratio of TiO_2/Al_2O_3 in all 07 aquifer sand samples [Table 4] which also reflects the extensive degree of chemical weathering in the study area.

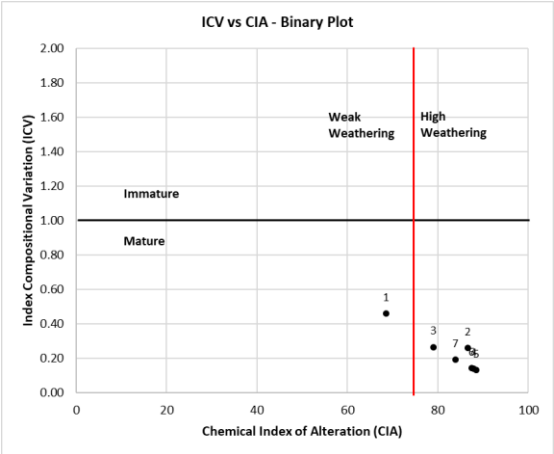

Fig. 4. ICV vs CIA binary plot [Baiyegunhi et al., 2017] of aquifer sand samples

Chemical Maturity

Sediment chemical maturity can be determined by estimating the index compositional variation (ICV) proposed by [Cox et al., 1995] which is calculated as $(Fe_2O_3+K_2O+Na_2O+CaO+MgO+MnO)/Al_2O_3$. The ICV tends to be highest in minerals that are high in weathering intensity and decreases in more stable minerals (less weathered minerals) [Baiyegunhi et al., 2017]. The sediments having ICV values greater than 1 are considered as compositionally immature while mature sediments have ICV values less than 1 [Cox et al., 1995]. The ICV values [Table 4] for the studied aquifer samples range between 0.13-0.46 which indicates that the coal seam roof aquifer layer is composed of chemically matured sand sediments. The ICV vs CIA binary plot [Baiyegunhi et al., 2017] also reveals that aquifer sand samples are chemically matured and experienced highest intensity of chemical weathering [Fig. 4].

Table 4 Elemental oxide concentrations in wt. % of aquifer sand samples, Thar Coal Block II

Parameters	Upper		Middle			Lower		Mean (%)
	Zone - A Sample 01	Zone - B Sample 02	Zone - C Sample 03	Zone - D Sample 04	Zone - E Sample 05	Zone - F Sample 06	Zone - G Sample 07	
SiO_2 (%)	85.27	56.47	76.05	59.62	52.05	50.15	47.72	60.05
TiO_2 (%)	0.78	2.53	1.35	2.35	1.96	2.17	1.55	1.81
Al_2O_3 (%)	9.55	31.83	17.86	33.40	39.36	40.21	38.49	30.01
Fe_2O_3 (%)	BDL	3.35	BDL	BDL	BDL	BDL	BDL	0.48
MgO (%)	BDL	BDL	BDL	BDL	BDL	BDL	BDL	BDL
CaO (%)	2.14	1.98	1.97	1.80	1.93	1.77	1.57	1.88
Na_2O (%)	0.31	0.87	1.02	1.16	1.48	2.35	4.49	1.67
K_2O (%)	1.94	2.07	1.74	1.67	1.76	1.62	1.35	1.74
Cl (%)	BDL	0.90	BDL	BDL	1.46	1.74	4.84	1.28
CIA	68.48	86.60	79.04	87.82	88.40	87.50	83.87	83.10
ICV	0.46	0.26	0.27	0.14	0.13	0.14	0.19	0.23
TiO_2/Al_2O_3	8.16	7.94	7.56	7.04	4.99	5.39	4.02	6.44
K_2O/Na_2O	6.22	2.38	1.70	1.44	1.19	0.69	0.30	1.99

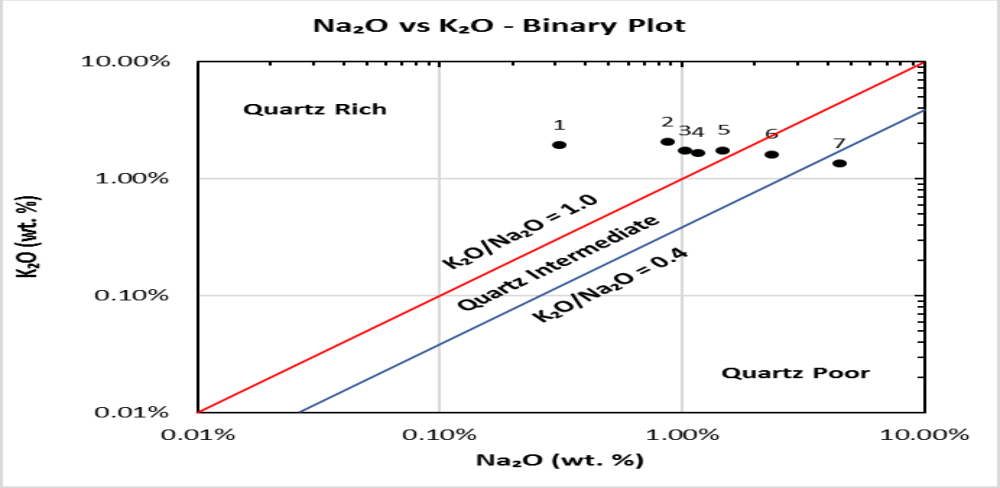

Fig. 5. Na_2O vs K_2O binary plot [after Crook, 1974] of aquifer sand samples

Mineralogy

Various binary and tertiary plots have been used to assess the coal seam roof aquifer sand mineralogy. Field investigations indicate that the aquifer sand is rich in fine to medium grain quartz with minor amount of clay and feldspar minerals.

K_2O vs Na_2O Binary Plot

Aquifer sand samples were plotted K_2O vs Na_2O binary plot [after Crook, 1974] to classify the samples based on its quartz richness [Fig. 5]. The results indicate that samples from upper and middle zones prove out to be quartz rich having K_2O/Na_2O ratio of greater than 1.00 while on

the other hand, samples from zone F and G fall under quartz intermediate and poor category having K_2O/Na_2O ratio less than 1.00 respectively [Table 4]. Na_2O vs K_2O plot demonstrates very clear mineralogical trend showing the gradual decline in quartz richness from upper to the lower zone of aquifer layer confirming the regional stratigraphic transformation of aquifer sand to carbonaceous claystone.

A-CN-K Ternary Plot

The CIA values of aquifer sand samples were plotted in Al_2O_3–(CaO* + Na_2O)–K_2O i.e. A–CN–K ternary plot [Nesbitt & Young, 1982] to idealize the presence of clay and feldspar minerals in aquifer sand samples. The ternary plot [Fig. 6] suggests that sample 1 (uppermost) shows fair amount of feldspar minerals while remaining sand samples indicates relatively higher amount of clay minerals (kaolinite, smectite, illite and chlorite) indicating intense chemical weathering in the area. Moreover, most of the aquifer sand samples fall along the A-CN line instead of A-K. This type of trend is generally found in sedimentary rocks that have undergone CN-metasomatism, by which addition of CN to weathered residues occurs [Fedo et al., 1995; Nagarajan et al., 2007]. Obviously, the highest degree of alteration (in terms of CIA) is compatible with samples high in kaolinite and low in feldspar content.

Log (SiO_2/Al_2O_3 vs Log (Na_2O/K_2O) Binary Plot

Coal seam roof aquifer sand samples have been further classified based on Log (SiO_2/Al_2O_3) vs Log

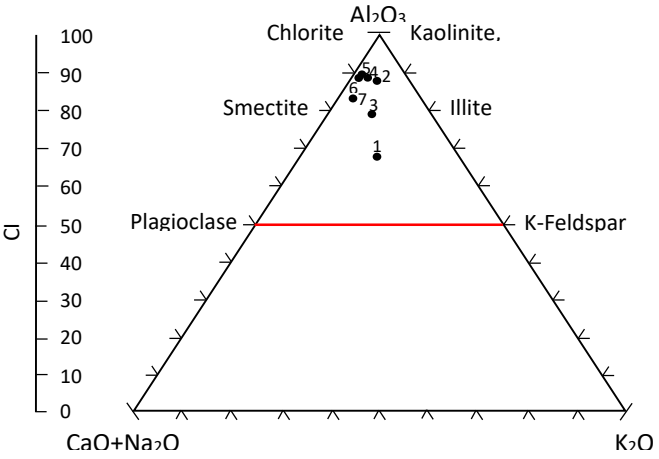

Fig. 6. A-CN-K ternary plot [Nesbitt & Young, 1982] of aquifer sand samples

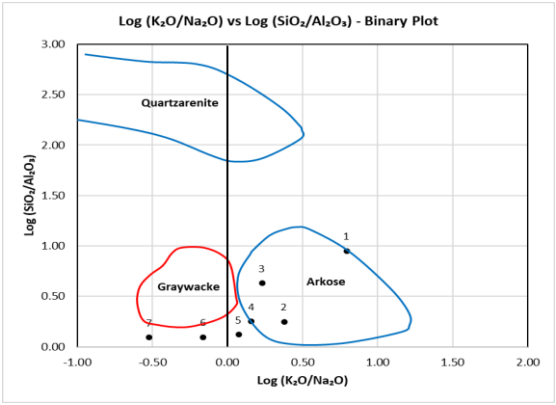

Fig. 8. Log (K_2O/Na_2O) vs Log (SiO_2/Al_2O_3) binary plot [Lindsey, 1999] of sand samples

(Na_2O/K_2O) binary plot classification scheme [Pettijohn et al., 1972]. The plot [Fig. 7] reveals identical mineralogical information that apart from sample 1 (uppermost zone) which falls under arkose category (contains at least 25% feldspar), all the remaining samples were classified as greywacke (contains more than 10% clay minerals). This indicates the progressive alteration of plagioclase and potassium feldspars to clay minerals which is also evident from the high CIA values from upper zone to the lower most zone of aquifer layer.

4.3.4. Log (K_2O/Na_2O) vs Log (SiO_2/Al_2O_3) Binary Plot

Based on the sandstone classification binary plot [Log (SiO_2/Al_2O_3) vs Log (K_2O/Na_2O)] of Lindsey, 1999, [Fig. 8]; aquifer sand sample 01 to 05 were categorized as arkose (contains at least 25% feldspar) while sample 06 and 07 were characterized as greywacke (contains more than 10% clay minerals) indicating similar mineral transformation trend (feldspar to clay) in aquifer layer from top to bottom as demonstrated from Fig. 7.

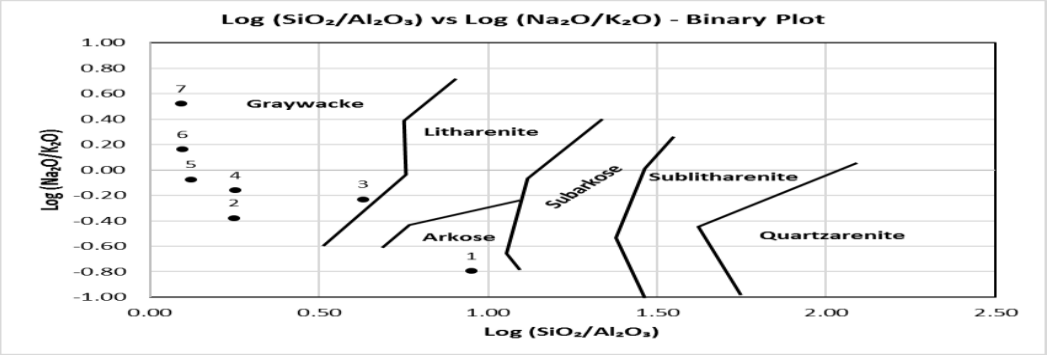

Fig. 7. Log (SiO_2/Al_2O_3) vs Log (Na_2O/K_2O) binary plot [Pettijohn et al., 1972] of aquifer sand samples

Na_2O-(Fe_2O_3+MgO)-K_2O Ternary Plot

The presence and enrichment of feldspar minerals in coal seam roof aquifer layer have been predicted using the Na2O-(Fe2O3+MgO)-K2O ternary plot proposed by Blatt et al., 1972. Fig. 8 reveals high percentage of K2O content in the upper and middle zone samples of aquifer layer while it transforms into Na2O content in the lower zone of aquifer layer. This elemental transformation from top to bottom of the aquifer layer suggest the alteration of potash feldspar into plagioclase feldspar and clays due to increased chemical weathering and maturity. Presence is ferro-magnesian potassic mineral is only recorded in sample 02 due to its high Fe2O3 content (upper zone).

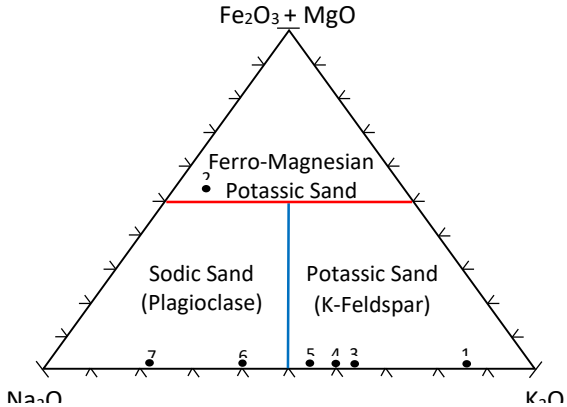

Fig. 9. Na_2O-(Al_2O_3+MgO)-K_2O ternary plot [Blatt et al., 1972] of aquifer sand samples

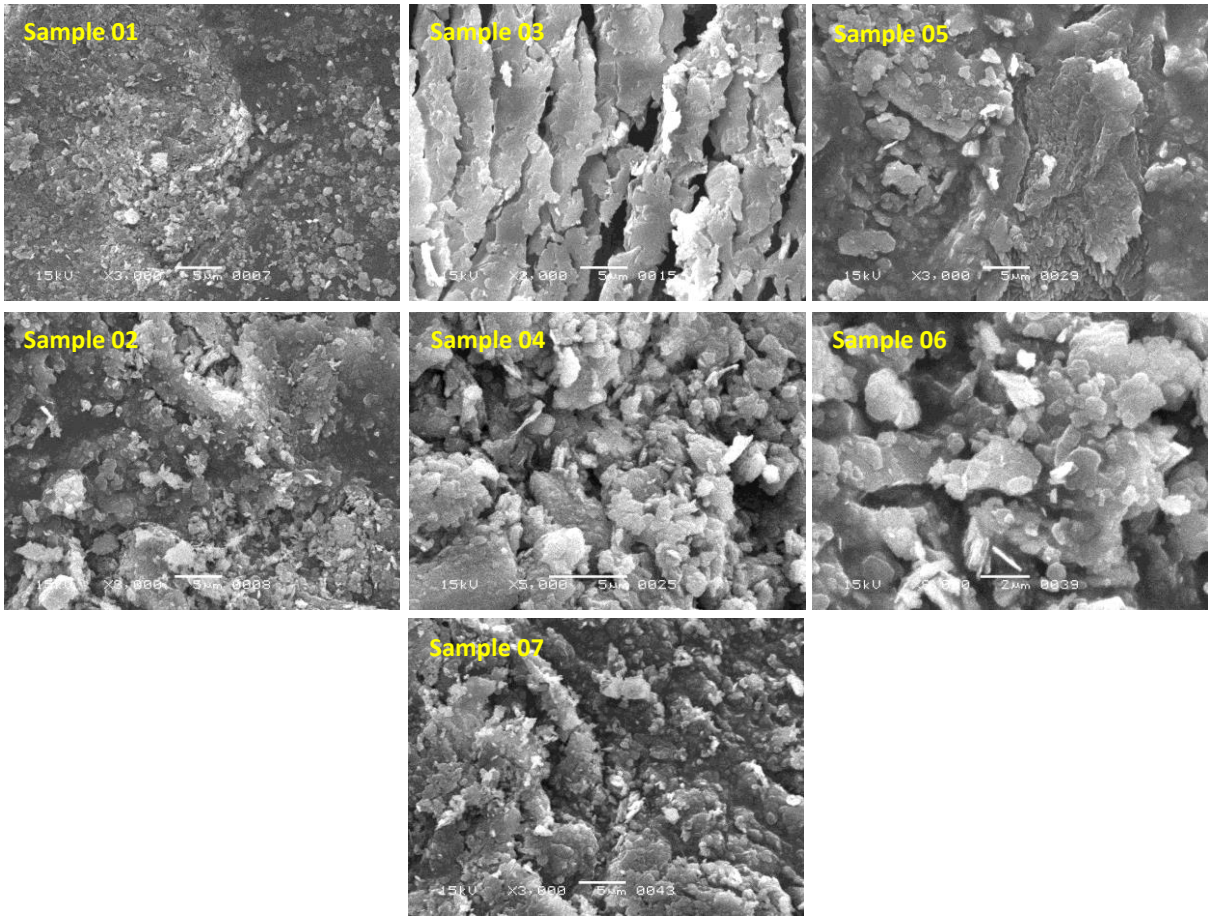

Fig. 10. Scanning Electron Microscope (SEM) images of aquifer sand samples, Thar Coal Block II

Industrial Applications

There are number of requirements which silica sand deposits must meet to be considered as potential source for different industrial applications [Platias et al., 2014] such as glass production, foundry sand, ceramics, sand blasting and other abrasive, building products, filter and extender, production of silicon and silicon carbide, pigments, hydraulic fractures and propping in oil industry and water filtration.

Table 5 demonstrates the chemical specifications of silica sand based on glass [British Standard – BS2975] and silicon semi-conductor industry [Xakalashe and Tangstad, 2011]. As per the standard, the initial Fe_2O_3 content of the silica sand must be approximately 0.13% whereas aluminium, magnesium, calcium and potassium presence affect the melting properties and must be kept at low levels [Platias et al., 2014].

Silica Purification

As per the raw silica content of upper, middle and lower zones of coal seam roof aquifer layer [Table 5], the upper zone shows the highest SiO_2 content of 70.87% while the middle and lower zone contains

62.57% and 48.93% of SiO_2 content respectively. The silica content of aquifer sand shall be enhanced/purified in order to utilize the coal seam roof aquifer layer industrially and commercially.

Impurities usually present in the silica sand are free and coated iron oxides, clay and smaller amounts of sodium, potassium and calcium minerals [Sundararajan et al., 2009]. Several investigations were carried out by various authors to remove Fe, Al and other impurities from silica sand in order to enhance the silica grade. The silica beneficiation techniques like wet sieving, magnetic separation, froth flotation and chemical leaching are some of the commonly practiced techniques for the removal of impurities from raw silica sand [Boussa et al., 2016]. However, physical separation techniques, such as froth flotation or magnetic separation, are generally less effective for impurities removal than chemical leaching [Tuncuk et al., 2013] where past experiments verified that the sulfuric acid is one of the best leaching agents for the removal of iron and aluminium impurities from the quartz sand, due the properties of H_2SO_4 which can enhance the SiO_2 content up to the desired industrial and commercial level [Boussa et al., 2016].

Table 5 Typical chemical specifications of glass [BS2975, 9] and silicon semi-conductor industry [Xakalashe and Tangstad, 2011]

Product		Grade	SiO_2 (%)	Fe_2O_3 (%)	Al_2O_3 (%)
Optical Glass		A	99.7	0.013	0.2
Tableware Glass		B	99.6	0.01	0.2
Borosilicate Glass		C	99.6	0.01	0.2
Colorless Container		D	98.8	0.03	0.1
Flat Glass		E	99.0	0.1	0.5
Colored Container		F	97.0	0.25	0.1
Insulting Fibers		G	94.5	0.3	3.0
Sheet Rolled and Polished Glass		-	89.5	0.06	0.5
Soda Lime		-	72.2	0.1	1.00
Metallurgical Silicon		18	99.00	0.2 – 0.3	1.5 – 4.0
Solar Silicon		7 and 19	99.99	<0.3	<0.1
Poly-Crystalline Solar Silicon		21	99.99	-	-
Electronic Silicon		19	99.99	<0.01	<0.0008
Studied Coal Seam Roof Aquifer Layer	**Upper Zone**	-	70.87	1.67	20.69
	Middle Zone	-	62.57	<0.01	30.21
	Lower Zone	-	48.93	<0.01	39.35
	Mean	-	**60.05**	**0.48**	**30.01**

SUMMARY AND CONCLUSIONS

A preliminary study was performed on Thar Block II coal seam roof aquifer layer based on grain size distribution, geochemistry and mineralogy to evaluate its industrial significance and

suitability. The coal seam roof aquifer layer is sub-divided into 07 vertical zones (A-G) in order to collect representative samples from top to bottom covering complete coal seam roof aquifer layer. The results of grain size analysis reveal that majority proportion of the studied aquifer samples (n=7) is mainly contributed of fine to medium grain sand while the aquifer layer permeability ranges from $6.32E^{-5}$-$3.60E^{-4}$m/s which is calculated from Beyer's equation. The uniformity coefficient (Cu) values indicates that the coal seam roof aquifer layer composed of well graded soil particles.

The geochemical analysis of the aquifer sand samples shows varying concentration of SiO_2 [47.72-85.27%] and Al_2O_3 [9.55-40.21%]. The uppermost zone A of aquifer layer contains highest SiO_2 content of 85.27% while it significantly reduces downward to the lowermost zone G showing least amount of SiO_2 content i.e. 47.72%. The high Chemical Index of Alteration (CIA) values of aquifer sand samples i.e. 79.04-88.40 indicate intensive chemical weathering in the study area and reflect that the coal seam roof aquifer sand has formed under tropical conditions. Similarly, the decreasing ratio of TiO_2/Al_2O_3 ratio (8.16-4.02) in studied samples also reflects the extensive degree of chemical weathering of aquifer layer. Moreover, the ICV vs CIA binary plot also reveals that aquifer sand samples are chemically matured and experienced highest intensity of chemical weathering.

Field investigations indicate that the aquifer sand is rich in fine to medium grain quartz with minor amount of clay and feldspar minerals. The K_2O vs Na_2O binary plot demonstrates very clear mineralogical trend showing the gradual decline in quartz richness from upper to the lower zone of aquifer layer confirming the regional stratigraphic transformation of aquifer sand to carbonaceous claystone. The A–CN–K ternary plot suggests that the uppermost zone A shows fair amount of feldspar minerals while remaining sand samples indicates relatively higher amount of clay minerals (kaolinite, smectite, illite and chlorite). The Log (SiO_2/Al_2O_3) vs Log (Na_2O/K_2O) binary plot classification scheme reveals identical mineralogical information that uppermost zone falls arkose category (contains at least 25% feldspar) while all the remaining samples were classified as greywacke (contains more than 10% clay minerals). The ternary plot Na_2O-(Fe_2O_3+MgO)-K_2O high percentage potash feldspar in the upper and middle zone samples of aquifer layer while it transforms into plagioclase feldspar in the lower zone of aquifer layer.

Since the SiO_2 content evaluated for coal seam roof aquifer layer is relatively less (upper = 70.87%, middle = 62.57% and lower = 48.93%) as per the standard industrial requirements, the SiO_2 content shall be enhanced/purified using chemical leaching techniques which are more effective for impurities removal than physical techniques such as wet sieving, froth flotation or magnetic separation.

ACKNOWLEDGEMENTS

The authors gratefully acknowledge the support of the management of Sindh Engro Coal Mining Company (SECMC), for granting permission to publish this paper. Authors are also thankful to Dr. Thomas von Schwarzenberg for his critical review of this paper.

Views expressed in this paper are that of the authors only and may not necessarily be of SECMC.

REFERENCES

Baiyegunhi, C., Liu, K., Gwavava, O., 2017. Geochemistry of Sandstones and Shales from The Ecca Group, Karoo Supergroup, In the Eastern Cape Province of South Africa: Implications For Provenance, Weathering and Tectonic Setting. Open Geosci. 9, 340-360.

Blatt, H., Middleton, G., Murray, R., 1972. Origin of Sedimentary Rocks. Englewood Cliffs, New Jersey, Prentice-Hall, 634 pp.

Boussaa, A.S., Kheloufi, A., Zaourar, N.B., Bouachma, S., 2016. Iron and Aluminium Removal from Algerian Silica Sand by Acid Leaching. Acta Physica Polonica Vol. 132, No. 3, 1082-1086.

Cox, R., Low, D.R., Cullers, R.L., 1995. The Influence of Sediment Recycling and Basement Composition on Evolution of Mudrock Chemistry in the Southwestern United States. Geochim. Cosmochim. Acta. 59 (14), 2919-2940.

Crook, K. A. W., 1974. Lithogenesis and Geotectonics: The Significance of Compositional Variation in Flysch Arenites (Graywackes). Soc. Econ. Paleontol, Mineral. Spec. Pub 19, 304–310.

DeGroot, D.J., Ostendorf, D.W., Judge, A.I., 2012. In Situ Measurement of Hydraulic Conductivity of Saturated Soils. Geotechnical Engineering Journal of the SEAGS & AGSSEA Vol. 43, No. 4, 63-72.

Fedo C.M., Nesbitt H.W., Young G.M., 1995. Unraveling the Effects of K Metasomatism in Sedimentary Rocks and Paleosols with Implications for Palaeoweathering Conditions and Provenance. J Geol. 23, 921–924.

Folk, R.L., 1951. Stages of Textural Maturity in Sedimentary Rocks. Journal of Sedimentary Petrology Vol. 21, 127-130.

Holtz, R.D., Kovacks, W.D., Sheahan, T.C., 2011. An Introduction to Geotechnical Engineering. Prentice-Hall, Upper Saddle River, NJ, 853 pp.

Jianmin, M., Xianliang, Z., Qiwen, H., 2010. Hydrogeological Exploration Study Report of Thar Desert, Block II, Sindh, Pakistan. China Northeast Coal Field Geological Survey Bureau, 1-182

Kazmi, A.H., 1985. Geology of the Thar desert, Pakistan. Acta Mineralogical Pakistan Vol. 1, 64-67.

Lindsey, D.A., 1999. An Evaluation of Alternative Chemical Classifications of Sandstones. USGS Open File Report, 23 pp.

Mitchell, J.K., and Soga, K., 2005. Fundamentals of Soil Behavior. John Wiley & Sons Inc., Hoboken, NJ, 592 pp.

Nagarajan, R., Madhavaraju, J., Nagendra, R., Armstrong-Altrin, J.S., Moutte, J., 2007, Geochemistry of Neoproterozoic Shales of the Rabanpalli Formation, Bhima Basin, Northern Karnataka, Southern India: Implications for Provenance and Paleoredox Conditions. Revista Mexicana de Ciencias Geológicas 24, 150-160.

Nedachi, Y., Nedachi, M., Bennett, G., Ohmoto, H., 2005. Geochemistry and Mineralogy of the 2.45 Ga Pronto Paleosols, Ontario, Canada. Chemical Geology 214, 21-44.

Nesbitt, H. W., Young, G. M., 1982. Proterozoic Climates and Plate Motion Inferred from the Major Element Chemistry of Lutites. Nature 299, 715-717.

Onur, E.M., 2014. Predicting the Permeability of Sandy Soils from Grain Size Distributions. Kent State University.

Pettijohn F. J., Potter P. E., Siever R., 1972. Sand and Sandstone; Berlin: Springer-Verlag. 241 pp.

Platias, S., Vatalis, K.I., Charalampides, G., 2014. Suitability of Quartz Sands for Different Industrial Applications. Procedia Economics and Finance 14, 491-498.

Rehman, M.U., Zaigham, N.A., Nizamani, M.A., Ahmad, M., Huda, Q. U., 1993. Coal Exploration in Tharparkar, Sindh, Pakistan. Geol. Survey of Pakistan, Record No. 95, 35 pp.

Scheffler, K., Hoernes, S., Schwark, L., 2003. Global Changes during Carboniferous-Permian Glaciation of Gondwana; Linking Polar and Equatorial Climate Evolution by Geochemical Proxies. Geology 31, 605-608.

Sundararajan, M., Ramaswamy, S., Raghavan, P., 2009. Evaluation for the Beneficiability of White Silica Sands from the Overburden of Lignite Mine situated in Rajpardi district of Gujarat, India. Journal of Minerals & Materials Characterization & Engineering Vol. 8, No. 9, 701-713.

Tuncuk, A., Ciftlik, S., Akcil, A., 2013. Hydrometallurgy 80, 134–135.

Xakalashe, B.S., Tangstad, M., 2011. Silicon Processing from Quartz to Crystalline Silicon Solar Cells. Southern African Pyrometallurgy, 83-100.